Preprint
UCRL-JC-142526

Update on Calibration of the Lawrence Livermore National Laboratory Passive-Active Neutron Drum Shuffler for Measurement of Highly Enriched Uranium Oxide

M. Mount, W. O'Connell, C. Cochran, P. Rinard, D. Dearborn, E. Endres

U.S. Department of Energy
Lawrence Livermore National Laboratory

This article was submitted to
43rd Annual Institute of Nuclear Material Management Meeting, Orlando, FL., June 23-27, 2002

May 17, 2002

This work was performed under the auspices of the United States Department of Energy by the University of California, Lawrence Livermore National Laboratory under contract No. W-7405-Eng-48.

Update on Calibration of the Lawrence Livermore National Laboratory Passive-Active Neutron Drum Shuffler for Measurement of Highly Enriched Uranium Oxide

Mark Mount, Lawrence Livermore National Laboratory
7000 East Avenue, L-347, Livermore, CA 94550, USA (925) 422-9800
William O'Connell, Lawrence Livermore National Laboratory
7000 East Avenue, L-195, Livermore, CA 94550, USA (925) 422-8789
Curtis Cochran, Lawrence Livermore National Laboratory
7000 East Avenue, L-347, Livermore, CA 94550, USA (925) 422-8542
Phillip Rinard, Los Alamos National Laboratory
Nuclear Safeguards Technology, MS E540, Los Alamos, NM 87545, USA (505) 667-2447
David Dearborn, Lawrence Livermore National Laboratory
7000 East Avenue, L-347, Livermore, CA 94550, USA (925) 424-6974
Eileen Endres, Lawrence Livermore National Laboratory
7000 East Avenue, L-347, Livermore, CA 94550, USA (925) 423-6630

Abstract

In October of 1999, Lawrence Livermore National Laboratory (LLNL) began an effort to calibrate the LLNL passive-active neutron (PAN) drum shuffler for measurement of highly enriched uranium (HEU) oxide. A single unit of certified reference material (CRM) 149 [Uranium (93% Enriched) Oxide - U_3O_8 Standard for Neutron Counting Measurements] was used to (1) develop a mass calibration curve for HEU oxide in the nominal range of 393 g to 3144 g ^{235}U, and (2) perform a detailed axial and radial mapping of the detector response over a wide region of the PAN shuffler counting chamber. Results from these efforts were reported at the Institute of Nuclear Materials Management 41st Annual Meeting in July 2000. This paper describes subsequent efforts by LLNL to use a unit of CRM 146 [Uranium Isotopic Standard for Gamma Spectrometry Measurements] in consort with Monte Carlo simulations of the PAN shuffler response to CRM 149 and CRM 146 units and a selected set of containers with CRM 149-equivalent U_3O_8 to (1) extend the low range of the reported mass calibration curve to 10 g ^{235}U, (2) evaluate the effect of U_3O_8 density (2.4 g/cm^3 to 4.8 g/cm^3) and container size (5.24 cm to 12.17 cm inside diameter and 6.35 cm to 17.72 cm inside height) on the PAN shuffler response, and (3) develop mass calibration curves for U_3O_8 enriched to 20.1 wt% ^{235}U and 52.5 wt% ^{235}U.

Calibration Plan

Since October 1999, a significant effort has been underway at the Lawrence Livermore National Laboratory (LLNL) to calibrate the LLNL passive-active neutron (PAN) drum shuffler for measurement of highly enriched uranium (HEU) oxide. The components of the calibration plan include (1) the replicate measurement of standards [certified reference materials (CRMs)] and working reference materials (WRMs), (2) Monte Carlo simulations of the PAN shuffler response to the standards and WRMs, (3) Monte Carlo simulations of

This work was performed under the auspices of the U.S. Department of Energy by the University of California, Lawrence Livermore National Laboratory under Contract No. W-7405-Eng-48.

the PAN shuffler response sensitivity to variations in U_3O_8 density, container diameter, and ^{235}U enrichment, and (4) the development of a set of calibration algorithms and their associated errors.

Measurement of Standards and Working Reference Materials

The initial step in the measurement effort was reported earlier [1] and involved the use of a unit of CRM 149 [Uranium (93% Enriched) Oxide - U_3O_8 Standard for Neutron Counting Measurements] to (1) develop a preliminary mass calibration curve for HEU oxide in the nominal range of 393 g to 3144 g ^{235}U, and (2) perform a detailed axial and radial mapping of the detector response over a wide region of the PAN shuffler counting chamber. Subsequent steps included the replicate measurement of (1) a unit of CRM 146 [Uranium Isotopic Standard for Gamma Spectrometry Measurements] to establish the PAN shuffler response to differences in ^{235}U enrichment and (2) two HEU metal WRMs to enhance validation of the Monte Carlo simulations. Table 1 summarizes the pertinent mass and ^{235}U enrichment information for the standards and WRMs used by LLNL in calibration of the PAN shuffler.

Table 1. Pertinent mass and ^{235}U enrichment information for the LLNL units of CRM 146 and CRM 149 [2, 3] and HEU metal WRMs.

LLNL Nomenclature	Material type	Total mass (g)	U mass (g)	^{235}U wt% (%)	^{235}U mass (g)	^{238}U mass (g)
CRM146-20	U_3O_8	230.01	194.48	20.107	39.10	154.70
CRM146-52	U_3O_8	230.00	193.86	52.488	101.75	90.87
CRM146-93	U_3O_8	230.05	194.44	93.1703	181.16	10.80
CRM149-05	U_3O_8	500.00	421.72	93.1959	393.03	22.75
CRM149-10	U_3O_8	999.80	843.28	93.1959	785.90	45.49
CRM149-15	U_3O_8	1499.93	1265.12	93.1959	1179.04	68.24
CRM149-20	U_3O_8	2000.23	1687.10	93.1959	1572.30	91.00
MRF004334	U metal	2299.4[1]	2296.0	93.180	2139.41	124.14
CRM149-30	U_3O_8	3000.07	2530.41	93.1959	2358.23	136.49
MRF004335	U metal	3070.3[1]	3065.0	93.170	2855.66	165.95
CRM149-40	U_3O_8	3999.37	3373.26	93.1959	3143.74	181.95

1. Includes the mass of the Ni-plated surface.

Monte Carlo Simulations of PAN Shuffler Response to Standards and Working Reference Materials

Monte Carlo simulations of the PAN shuffler response to the standards and WRMs were performed with the MCNP code [4] using the technique and post-processor developed by Rinard [5]. Models of the standards and WRMs used in the MCNP simulations reflected the appropriate U_3O_8 and U metal densities (3.18 g/cm^3 for the unit of CRM 146, 2.4 g/cm^3 for the unit of CRM 149, and 18.6 g/cm^3 for the two metal WRMs) and were true to the packaging of each, including the primary containers and any packing materials (Al foil) and secondary (over-pack) containers required to satisfy LLNL Plutonium Facility containment requirements. Table 2 summarizes the comparison of MCNP simulated and measured delayed neutron count rates for the standards and WRMs used by LLNL in calibration of the PAN shuffler.

Table 2. Comparison of MCNP simulated and measured delayed neutron count rate results for the LLNL units of CRM 146 and CRM 149 and HEU metal WRMs.

LLNL Nomenclature	Simulated count rate ^{235}U (counts/s)	Simulated count rate ^{235}U and ^{238}U (counts/s)	Measured count rate (counts/s)	Simulated to measured ratio
CRM146-20	69.22 ± 0.76	86.83 ± 0.77	86.49 ± 1.42	1.004 ± 1.87%
CRM146-52	154.27 ± 1.47	165.25 ± 1.47	165.70 ± 2.28	0.997 ± 1.64%
CRM146-93	246.00 ± 2.11	247.40 ± 2.11	240.91 ± 1.34	1.027 ± 1.02%
CRM149-05	558.94 ± 3.24	561.92 ± 3.24	557.19 ± 6.19	1.008 ± 1.25%
CRM149-10	993.20 ± 4.85	999.34 ± 4.85	1000.88 ± 5.14	0.998 ± 0.71%
CRM149-15	1403.90 ± 6.12	1413.27 ± 6.12	1411.18 ± 5.21	1.001 ± 0.57%
CRM149-20	1808.91 ± 7.25	1821.56 ± 7.25	1824.29 ± 6.81	0.998 ± 0.55%
MRF004334	2379.69 ± 8.86	2399.48 ± 8.86	2365.76 ± 10.12	1.014 ± 0.57%
CRM149-30	2614.55 ± 9.29	2633.94 ± 9.29	2650.21 ± 8.54	0.994 ± 0.48%
MRF004335	2947.62 ± 10.58	2975.70 ± 10.58	2954.69 ± 10.29	1.007 ± 0.50%
CRM149-40	3404.53 ± 11.19	3430.62 ± 11.19	3459.95 ± 8.62	0.992 ± 0.41%
			Average	1.004 ± 1.01%

From the ratios of the simulated to measured count rates, it follows that the appropriateness of Monte Carlo simulations as a tool in the PAN shuffler calibration process is validated: the maximum and minimum in the ratios are 1.027 ± 1.02% (CRM146-93) and 0.992 ± 0.41% (CRM149-40), respectively, a difference of only 3.5%; while the average of the ratios, including those for the two HEU metal WRMs, is a remarkable 1.004 ±1.01%.

Monte Carlo Simulations of PAN Shuffler Response Sensitivity to Variations in U_3O_8 Density, Container Diameter, and ^{235}U Enrichment

In order to determine the sensitivity of the PAN shuffler response to variations in U_3O_8 density, container diameter, and ^{235}U enrichment, an extensive series of MCNP simulations were performed. Response sensitivities to variations in U_3O_8 density and container diameter were evaluated for five different densities (2.4 g/cm^3, 3.0 g/cm^3, 3.6 g/cm^3, 4.2 g/cm^3, and 4.8 g/cm^3) and six different primary containers that bracket the range in size of those used at LLNL (tomato paste can, half-pint paint can, pint paint can, Kaufman can, quart can, and CRM 149 can) using U_3O_8 of an elemental and isotopic composition (93.1959 wt% ^{235}U) equal to that of the LLNL unit of CRM 149 and mass range that varied in irregular increments from a minimum of 10 g to the nominal maximum for the primary container and density under evaluation. Table 3 summarizes the pertinent information for the primary containers used by LLNL in the PAN shuffler response sensitivity study.

Response sensitivities to variations in ^{235}U enrichment were evaluated for (1) five different densities (2.4 g/cm^3, 3.0 g/cm^3, 3.6 g/cm^3, 4.2 g/cm^3, and 4.8 g/cm^3) in one primary container (CRM 149 can) using U_3O_8 of an elemental and isotopic composition (20.107 wt% ^{235}U, 52.488 wt% ^{235}U, and 93.1703 wt% ^{235}U) equivalent to that of the LLNL unit of CRM 146, and (2) one density (3.0 g/cm^3) in three different primary containers (tomato paste can, half-pint paint can, and pint paint can) using U_3O_8 of an elemental and isotopic composition (20.107 wt% ^{235}U and 52.488 wt% ^{235}U) equal to that of the LLNL unit of CRM 146. The mass

range again varied in irregular increments from a minimum of 10 g to the nominal maximum for the primary container and density under evaluation.

Table 3. Pertinent information for the primary containers used in the PAN shuffler response sensitivity study.

Primary container	Material of construction	Inside diameter (cm)	Inside height (cm)
Tomato paste can	Low carbon steel	5.24	6.99
Half-pint paint can	Low carbon steel	6.99	6.35
Pint paint can	Low carbon steel	8.26	8.57
Kaufman can	Low carbon steel	8.57	9.60
Quart can	Low carbon steel	9.88	13.29
CRM 149 can	304L stainless steel	12.17	17.72

As was the case with the models of the standards and WRMs, the sensitivity models used in the MCNP simulations were true to the packaging of each, including the primary containers, packing materials (Al foil for the CRM 149 can and polyvinylchloride bag-out bag and polyethylene poultry bag for all other containers), and secondary (over-pack) containers required to satisfy LLNL Plutonium Facility containment requirements.

Calibration Algorithms and Error Modeling

The earlier calibration [1] is extended to a broader range of mass, density, container diameter, and ^{235}U enrichment using the MCNP simulations just described. A functional and curve fitting process is used for interpolation and modest extrapolation. The goal is to fit closely to the MCNP results and to have a functional form suitable for interpolation between the MCNP cases. The equation forms for the curves are guided by some of the physics in the measurement process. Similarl to other neutron-based measurements [6] there are effects of attenuation, self-shielding, and multiplication.

The qualitative features of the irradiation and counting process are seen in the series of MCNP results. As evidenced most prominently in Figure 1, the delayed neutron count rate increases almost linearly with ^{235}U mass, while effects from other parameters are seen in the family of curves. For a given mass, count rate varies over a range of more than ± 10% depending on density and container diameter, and over a greater range depending on enrichment. Similarly, when using the curves in the inverse direction to determine the mass from a count rate, there are variations in mass of more than ± 10%. These variations are seen more clearly in Figure 2 in the plots of count rate per unit mass of ^{235}U.

The MCNP simulations provide further detail on the production and detection of delayed neutrons and are in two steps — the number of fissions of each isotope and hence the delayed neutrons created for an irradiation, and the detector efficiency for delayed neutrons. The post-processor [5] provides for the time-dependent properties of the delayed neutrons. The size of the attenuation, self-shielding, and multiplication effects all depend on the thickness of uranium material a neutron encounters, between the irradiation source and the uranium atoms in the sample, or between the origin points of the delayed neutrons and the exterior of the sample on the way to the detector. Hence we use the ^{235}U linear density of the sample as an independent variable. We use a distance between the exterior and the center point of the sample as a representative distance. The PAN shuffler irradiation sequence irradiates the sample from a wide range of angular directions,

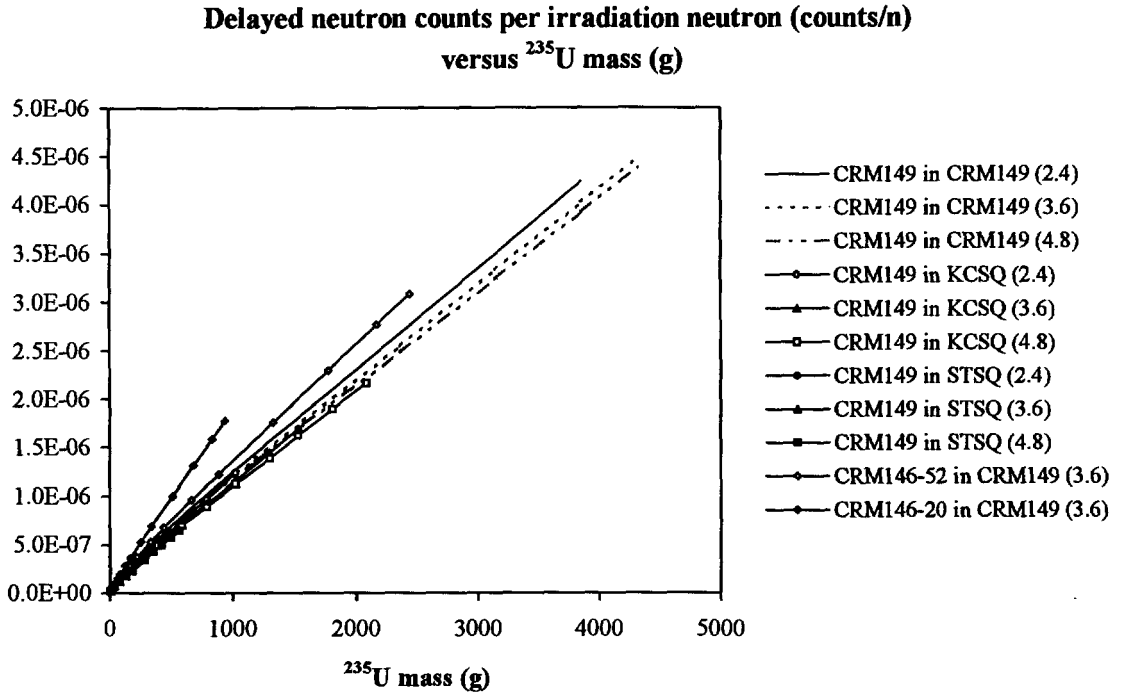

Figure 1. Delayed neutron counts per irradiation neutron, versus ^{235}U mass, for selected container and U_3O_8 conditions. The masses range up to the maximum that can fit in a particular can at the particular density and enrichment. In the chart legend, the first text item identifies the material (see Table 1), the second text item identifies the primary container (CRM149 means a CRM 149 can, KCSQ means a Kaufman can, and STSQ means a tomato paste can), and the third text item identifies the U_3O_8 density in g/cm^3.

so choosing a representative angle is necessarily an approximation. We give greater weight to the angles with a shorter distance to the center. This is appropriate for ^{235}U because the fissions per unit mass are highest with the least self-shielding. For an irradiation direction entering the top of the U_3O_8-filled cylindrical mass within the container, we define a path L_T, in cm, to the center point of the U_3O_8 mass with a direction of 45° (or an angle to the corner of the cylinder if the height exceeds the diameter). Thus,

$$L_T = \text{minimum} \left[\frac{0.5 \times H_{PC} \times \sqrt{2}}{\sqrt{(0.5 \times H_{PC})^2 + (R_{PC})^2}} \right] \quad (1)$$

where H_{PC} and R_{PC} are the inside height and inside radius, in cm, of the primary container, respectively.

For an irradiation direction entering the side of the U_3O_8 mass, we define a path L_S, in cm, entering the side at the 3/4 height to the exact center of the cylindrical mass. Thus,

$$L_S = \sqrt{(0.25 \times H_{PC})^2 + (R_{PC})^2} \quad (2)$$

For a nonlinear average favoring the smaller of the two lengths, we define the path length L, in cm, as the average of the inverses:

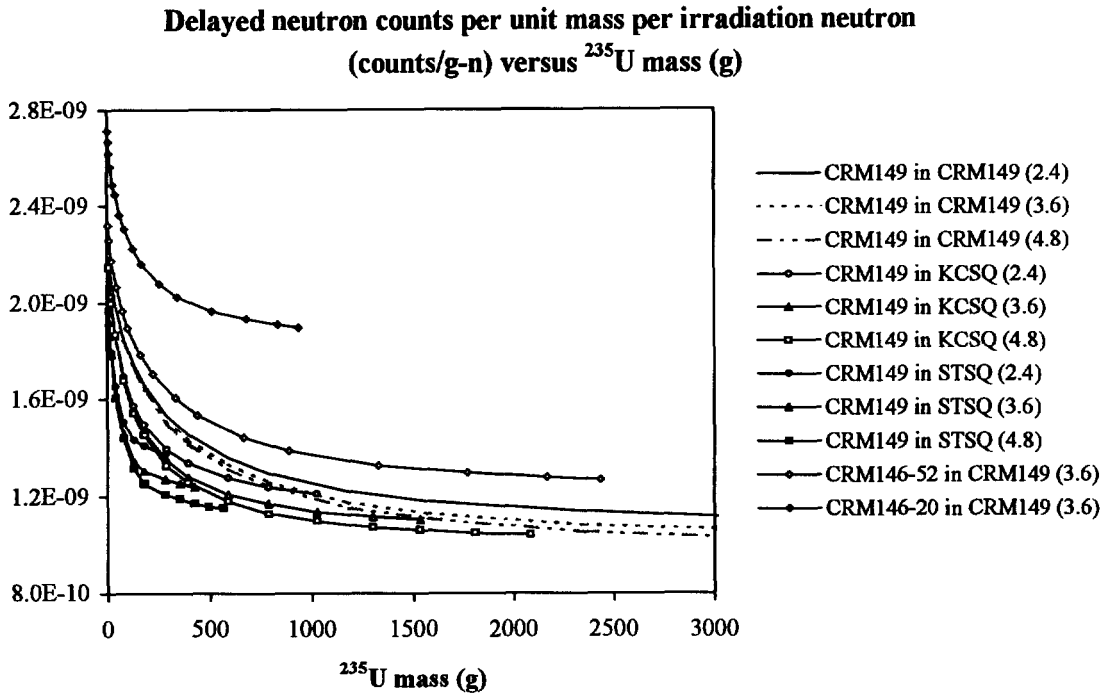

Figure 2. Delayed neutron counts per irradiation neutron per unit mass of ^{235}U, versus ^{235}U mass, for the selected container and U_3O_8 conditions. The CRM146-20 curve is the highest, and the CRM146-52 curve is second. For the CRM 149 material (93.1959 wt% ^{235}U), at low mass the curves are grouped by container size, with the curves for the larger-diameter cans being larger, thus in decreasing order, the CRM 149 can, the Kaufman can, and the tomato paste can. As mass increases, the curves diverge, with the smaller U_3O_8 mass density giving the larger response.

$$L = \frac{2}{(1/L_T + 1/L_S)} \tag{3}$$

The ^{235}U linear density $D_{L_{235_U}}$, in g/cm^2, is then given by

$$D_{L_{235_U}} = \rho_U \times Enr_{235_U} \times L \tag{4}$$

where ρ_U is the density of U in the U_3O_8, in g/cm^3, Enr_{235_U} is the fractional enrichment of ^{235}U, and all other terms are as previously defined.

Figure 3 shows the ^{235}U delayed neutron production rate per unit mass versus ^{235}U linear density as defined above. The curves versus linear density are much closer to a uniform curve. This supports the concept that linear density is an important explanatory concept. Now the curve fitting strategy suggests itself. Transform the production rate curves versus mass to curves versus linear density, fit the curves as a function of linear density, interpolate, and back-transform to the form versus mass.

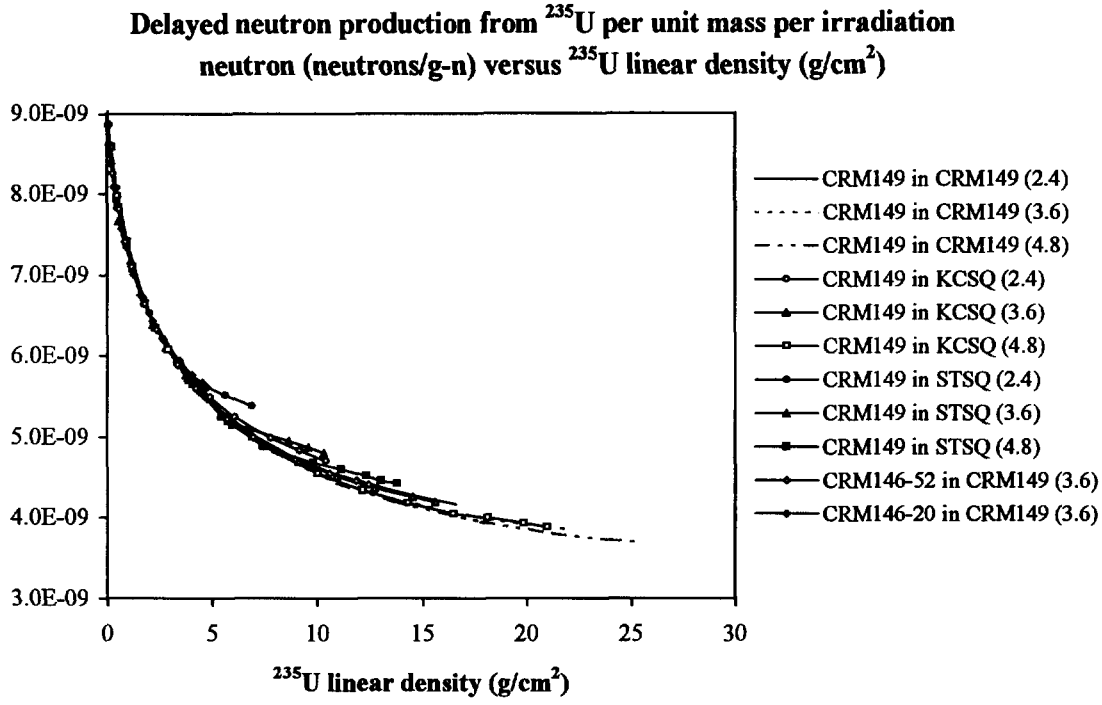

Figure 3. Delayed neutron production from only the ^{235}U in the sample, per irradiation neutron per unit mass of ^{235}U, versus ^{235}U linear density, for the selected container and U_3O_8 conditions. The variation between the curves is greatly reduced compared to Figure. 2. The variation is larger at the upper end of the individual curves, when the U_3O_8 fill height is larger than the diameter.

Figure 4 shows the ^{238}U fission production rate per unit mass of ^{238}U versus ^{235}U linear density. For a given series varying mass for a specified container and U_3O_8 density, the ^{238}U linear density and the U_3O_8 linear density are proportional to the ^{235}U linear density, hence the ^{235}U linear density is still a useful parameter. The curves are not as close to each other as in the ^{235}U case, with enrichment making the largest difference. Curve fitting and interpolation between curves can model this family of curves. The ^{238}U contributes between 0.3% and 25% of the total delayed neutron counts, depending mainly on enrichment and density, so the ^{238}U model is of some importance in the overall result.

Figure 5 shows the net detection efficiency versus ^{235}U linear density.

Figures 3-5 show constituent results versus a ^{235}U linear density. As mass and linear density increase, shielding and multiplication effects increase. For fissions and hence later neutron production rate from ^{235}U, a net self-shielding effect is evident. For fissions of ^{238}U, multiplication of the incoming irradiation neutrons is a strong effect (except at the lowest ^{235}U enrichment studied) because of the dependence of ^{238}U fission on neutrons of energy greater than about 1 MeV [Fig. 12.6, Ref 7]. For delayed neutrons emitted within the measured object and traveling toward the detectors, the multiplication is stronger than attenuation, leading to a net increase in counting efficiency with mass.

The ^{235}U delayed neutron production rate (as in Figure 3) as a function of ^{235}U linear density is fitted by three declining exponentials. A fairly smooth variation of the curve parameters as a function of U_3O_8 density, enrichment, and container diameter is achieved by placing some constraints on the parameter values for neighboring curves.

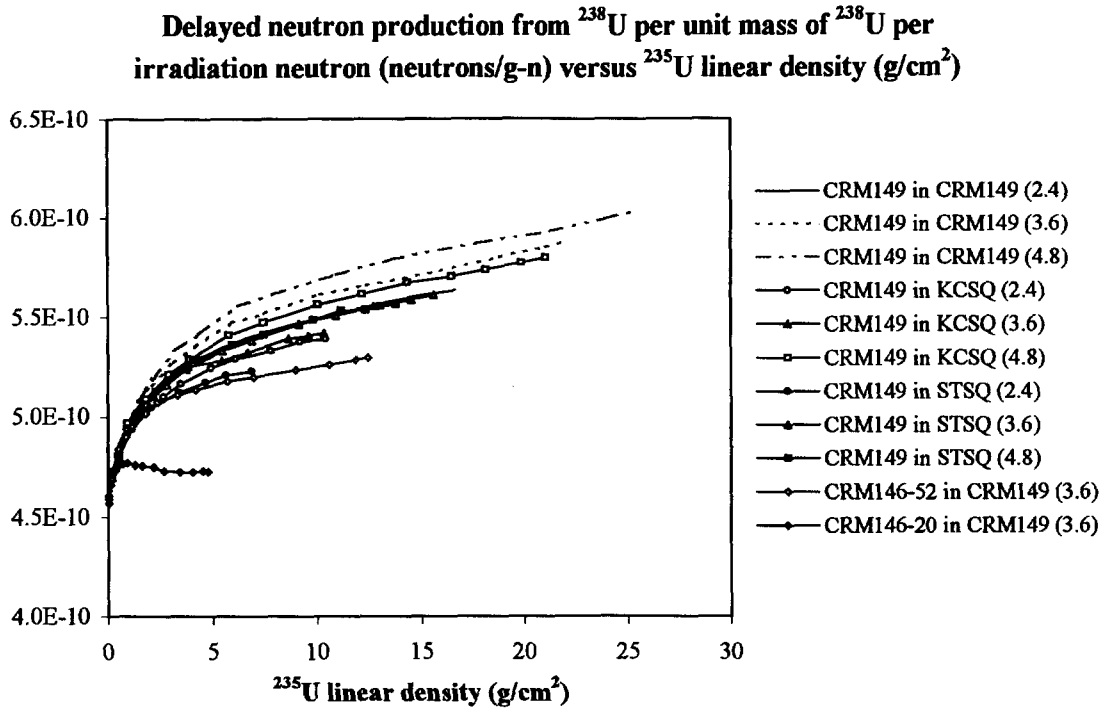

Figure 4. Delayed neutron production from only the ^{238}U in the sample, per irradiation neutron per unit mass of ^{238}U, versus ^{235}U linear density, for the selected container and U_3O_8 conditions.

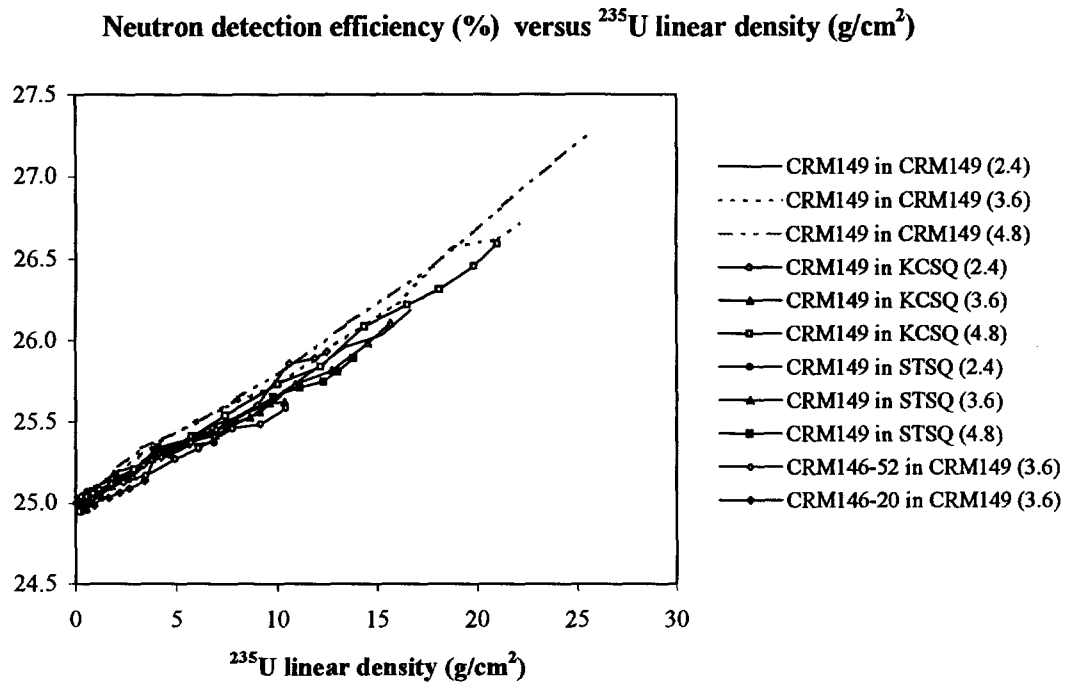

Figure 5. Net detection efficiency for delayed neutrons, versus ^{235}U linear density of the sample, for the selected container and U_3O_8 conditions.

For ^{238}U delayed neutrons vs ^{235}U linear density, a line plus a declining exponential is used. For detection efficiency a straight line is used for each case. The slope is found to be slightly greater for a greater ^{235}U mass density.

The curve parameters change slowly with the underlying variables of U_3O_8 density, enrichment, and container diameter, so interpolated curves can be constructed by linear interpolation of the curve parameters. Then the total delayed neutron counts per irradiation neutron can be calculated from the ^{235}U, ^{238}U, and efficiency constituents. Counts per irradiation neutron can be converted to counts per second by using the source strength calibration. Thus we can produce a calibration curve of counts per second versus ^{235}U mass for any container, enrichment, and U_3O_8 density within the covered range.

The count rate-to-mass calibration error is made up of several components. The MCNP simulations have a statistical error at one standard deviation of ± 0.5% to ± 1%. The fits adhere closely to the simulation results and so share in most of their error. The modeling error (equation to simulation result mismatch) is ± 0.5% to ± 2.6% depending on whether the interpolated container condition is close to the MCNP anchor points or not. There is also a systematic error of about ± 1% in the neutron source strength calibration. Thus the total error in application of the count rate-to-mass calibration is in a range from 1.2% to 3%.

Selected Unknown Item Measurement Results

Table 4 summarizes the measurement results for a selected set of LLNL unknown HEU oxide items chosen to demonstrate the applicability of the LLNL PAN shuffler HEU oxide calibration algorithms. These items cover an extensive range in container diameter (5.24 cm to 12.21 cm), declared mass (20 g to 4394 g), and declared enrichment (30.14 wt% ^{235}U to 93.20 wt% ^{235}U). Because the U_3O_8 density of each item was neither declared nor measured, all items were initially assumed to have a nominal U_3O_8 density of 2.4 g/cm^3. However, for those items whose measured U_3O_8 mass was calculated to exceed the capacity of its container, the U_3O_8 density was increased in increments of 0.1 g/cm^3 to the extent necessary for the container to accommodate the measured U_3O_8 mass.

Table 4. Summary of measurement results for selected LLNL unknown HEU oxide items.

Item Identification	Container diameter (cm)	U_3O_8 density (g/cm^3)	Declared U mass (g)	Declared ^{235}U wt% (%)	Measured U mass (g)	U mass difference (g)
MRF003439	5.24	2.4	20.00	75.78	14.79 ± 0.81	-5.21
MRF003420	8.26	2.4	80.00	93.00	86.01 ± 2.04	6.01
MRF004855	8.57	2.6	1224.00	93.19	1205.08 ± 21.25	-18.92
MRF003421	9.88	2.4	248.00	93.14	180.72 ± 4.02	-67.28
MRF005014	9.88	2.4	1605.64	92.93	1609.98 ± 28.37	4.34
MRF004677	9.88	2.4	1632.20	93.20	1574.13 ± 27.48	-58.07
MRF005021	9.88	3.0	2476.00	30.14	2511.27 ± 69.13	35.27
MRF003386	10.55	2.4	113.00	93.15	111.99 ± 2.23	-1.01
MRF003330	12.21	2.6	4394.00	93.15	4455.14 ± 76.19	61.14
				Total	11749.11 ± 112.35	-43.73

Because of the very nature of the items themselves (i.e., unknowns with experimenter declared values), the spread exhibited in the individual differences between the declared and measured U mass and the total U mass difference is not unexpected. While the measured U mass results reflect the accountability values for these items and are therefore not subject to an inventory difference analysis, the total U mass difference of -43.73 g is no more than 0.37% of the total measured U mass and well within the standard deviation (± 112.35 g) and the 95% confidence limit (± 222.45 g) in the total measured U mass.

References

[1] M. Mount, J. Glosup, C. Cochran, D. Dearborn, and E. Endres, "Calibration of the Lawrence Livermore National Laboratory Passive-Active Neutron Drum Shuffler for Measurement of Highly Enriched Uranium Oxide," in *Proceedings of the 41st Annual Meeting, Institute of Nuclear Materials Management*, New Orleans, LA, July 16-20, 2000.

[2] New Brunswick Laboratory, "Certified Reference Material Certificate of Analysis, CRM 146, Uranium Isotopic Standard for Gamma Spectrometry Measurements," New Brunswick Laboratory, Argonne, IL (July 30, 1999).

[3] New Brunswick Laboratory, "Certified Reference Material Certificate of Analysis, CRM 149, Uranium (93% Enriched) Oxide - U_3O_8 Standard for Neutron Counting Measurements," New Brunswick Laboratory, Argonne, IL (November 30, 1999).

[4] J. F. Briesmeister, Editor, *MCNP™ -- A General Monte Carlo N-Particle Transport Code, Version 4C*, LA-13709-M, Los Alamos National Laboratory, March 2000.

[5] P. M. Rinard, "Calculating Accurate Shuffler Count Rates with Applications," in *Proceedings of the 42nd Annual Meeting, Institute of Nuclear Materials Management*, Indian Wells, CA, July 15-19, 2001.

[6] N. Ensslin, "Principles of Neutron Coincidence Counting," Chap. 16 of *Passive Nondestructive Assay of Nuclear Materials*, US Nuclear Regulatory Commission, NUREG/CR-5550, and Los Alamos National Laboratory, LA-UR-90-732, March 1991.

[7] P. Rinard, "Neutron Interactions with Matter," Chap. 12 of *Passive Nondestructive Assay of Nuclear Materials*, US Nuclear Regulatory Commission, NUREG/CR-5550, and Los Alamos National Laboratory, LA-UR-90-732, March 1991.